ESTIMATION OF FORMATION PARAMETERS USING FULL WAVEFORM ACOUSTIC AND SHEAR WAVE LOGS

by

N.Y. Cheng and C.H. Cheng

Earth Resources Laboratory
Department of Earth, Atmospheric, and Planetary Sciences
Massachusetts Institute of Technology
Cambridge, MA 02139

ABSTRACT

A combination of borehole Stoneley waves from full waveform acoustic logs and direct shear wave logs was used to estimate formation permeability and shear wave velocity. Data sets used here were collected by ARCO's array full waveform acoustic logging tool and shear wave logging tool. The P- and S-wave velocities of the formation are determined by threshold detection with cross-correlation correction from the full waveform and the shear wave log, respectively. The full waveform acoustic logging data are also processed using the Extended Prony's method to estimate the borehole Stoneley wave phase velocity and attenuation as a function of frequency. Two different borehole models are considered for the inversion of Stoneley wave velocity and attenuation data. They are the isotropic elastic and the porous isotropic borehole models. Inversion parameters include shear wave velocity and formation permeability. Inverted shear wave velocities and permeabilities are compared with the shear wave log and the core permeability measurements, respectively, for an integrated interpretation and possible identification of shear wave anisotropy.

INTRODUCTION

Borehole acoustic logging can provide information about the in-situ physical properties of subsurface formation. The common approach is to estimate formation P-wave velocity by picking the first arrival from conventional log data. Since the advance of full waveform logs, we can determine the S-wave velocity in "hard" or "fast" formations, where the formation shear wave velocity is higher than the compressional wave velocity in the borehole fluid, by measuring the moveout of the shear/psuedo-Rayleigh wave packet. In "soft" or "slow" formations this is not possible because there is no refracted shear/psuedo-Rayleigh arrival. One can estimate the shear wave velocity by

inverting the Stoneley wave velocity (Cheng and Toksöz, 1983; Stevens and Day, 1986). However, this only really works in an isotropic elastic formation. More recently the advance of direct shear wave logging using the flexural mode of the borehole makes the direct measurement of shear wave velocity in "soft" formations possible (Zemanek et al., 1984). There is additional information contained in the Stoneley waves such as the permeability of the formation (Rosenbaum, 1974; Schmitt et al., 1988). Furthermore, anisotropy affects the different wavemodes differently. The shear wave log measures mainly the shear wave velocity in the vertical direction along the borehole, while the Stoneley mainly measures the shear wave velocity in the horizontal direction perpendicular to the borehole. Thus a combination of these measurements may allow us to further characterize the formation in terms of velocity anisotropy.

Propagation of the Stoneley wave in a fluid-filled borehole surrounded by an isotropic solid is well understood (Biot 1952; Cheng and Toksöz 1981). When the formation is a porous medium the situation becomes more complicated but more interesting. Williams et al. (1984) showed the strong correlation of in situ permeability with Stoneley wave velocity and attenuation. Since then several attempts have been made to obtain in situ permeability directly from full waveform acoustic logging data. Burns et al. (1988) applied the damped least square inversion to borehole Stoneley wave velocity and attenuation data to estimate in situ permeability. Stoneley wave dispersions were estimated from data collected by a tool with only two receivers. The forward model was based on the Biot-Rosenbaum model of wave propagation in a borehole in a porous formation (Biot, 1956a,b; Rosenbaum, 1974). The results were in reasonable agreement with the core measurements. The ultrasonic model laboratory experiments performed by Winkler et al. (1989) filled the gap between the Biot-Rosenbaum theory and field applications. The laboratory measured Stoneley wave velocity and attenuation in a permeable borehole were in excellent agreement with the predictions of the Biot-Rosenbaum model. Tang et al. (1991) formulated a simplified version of the Biot-Rosenbaum model dealing with the borehole Stoneley wave. It provides a clear physical picture of propagation of the Stoneley wave in the permeable borehole.

The phase velocities of the Stoneley wave are also affected by the mechanical properties of a transversely isotropic formation (White and Tongtaow 1981; Ellefsen 1990). In the case of a transversely isotropic formation with its symmetry axis parallel to the borehole, Stoneley wave phase velocity is sensitive to c_{66} at low frequency, and to c_{44} at high frequency. These sensitivities are the basis of the borehole Stoneley wave inversion in the transversely isotropic formation. However, these analyses are restricted to a borehole in line with the axis of symmetry of the transversely anisotropy formation. For a borehole normal to the axis of symmetry of an transversely anisotropic formation (creating a situation with azimuthal anisotropy), there is no analytic solution as of yet, but Ellefsen et al. (1991) have obtained numerical solutions for the phase velocity dispersion of the Stoneley wave using the Finite Element Method.

In this paper we process data from two sections of a borehole where both the array sonic log and shear wave log are available. The array data are processed using the Extended Prony's method to estimate the borehole Stoneley wave phase velocity and attenuation as a function of frequency. These are then inverted using the damped least-square method with Stoneley wave amplitude as a weighting function. Inverted shear wave velocities and permeabilities are compared with the shear wave log and the core permeability respectively.

DATA ANALYSIS AND INVERSION

Tool Geometry

The full waveform sonic logging data are collected by the ARCO array sonic tool with 12 receivers and two sources (Figure 1a). The distance between successive receivers is 6 inches. There are 512 points recorded at each receiver with a sampling rate of 11 μs. There is a 25 μs time delay between each trace. Shear wave logging data are collected by the ARCO dipole shear wave logging tool with two receivers located at 9 and 13.5 ft from the source (Figure 1b). This tool generates a dipole displacement field in the borehole which results in a flexural wave propagating down the borehole with the first arrival at the shear wave velocity. There are 1024 data points recorded at each receiver with a sampling rate of 11 μs. The tools collect data every half foot along the borehole. Figure 2 shows an iso-offset plot of the full waveform data through a section of the formation. The P-wave arrival and the low frequency Stoneley wave can be easily identified on the plot. Figure 3 shows the waveforms recorded at the near receiver of the shear wave tool. The shear/flexural mode arrival can be easily identified.

Data Processing

The full waveform sonic and shear wave data are processed first to determine the formation P- and S-wave velocities. In both cases the first arrivals are picked by threshold detection and then the picks are correlated across different receiver waveforms to pick the maximum correlation in the first arrival waveform between receivers. The formation P- and S-wave velocities are determined this way from the full waveform and shear wave logs, respectively.

Next the full waveform array sonic data are processed by the Extended Prony's method to estimate borehole Stoneley wave phase velocity and attenuation (Lang et al., 1987; Ellefsen et al., 1989). This method transforms the data from the time domain into the frequency domain, and then at each frequency, the spectral data at each receiver is fitted to a propagating wave mode (pseudo-Rayleigh or Stoneley) of the following form:

$$A(\omega)e^{-\alpha(\omega)z}e^{i(\phi(\omega)+k(\omega)z)} \tag{1}$$

where ω = angular frequency
           k = wavenumber of the propagating mode
           z = distance between source and receiver.
           $A(\omega)$ = amplitude of the incident wave at the first receiver
           $\phi(\omega)$ = phase of the incident wave at the first receiver
           $\alpha(\omega)$ = attenuation coefficient of the propagating mode

In this way, we can find the $A(\omega)$, $k(\omega)$, and $\alpha(\omega)$ which best fit the data by means of a least squares algorithm. The phase velocity is given by

$$c(\omega) = \frac{\omega}{k(\omega)}. \tag{2}$$

The attenuation coefficient, α, is sometimes alternately expressed as the imaginary part of the wavenumber k. Using the Extended Prony's method, the velocity dispersion and attenuation of the Stoneley wave as a function of frequency can be easily determined. The Stoneley wave velocity and attenuation data obtained here are the input data for the inversion.

Figure 4 shows one typical array of waveforms collected by receivers from the far source in the field. In the slow formation encountered here only P-wave arrivals and the Stoneley wave appear in the log. The frequency content of the Stoneley wave is much lower than the P wave. The results from the Extended Prony's Method processing are plotted in Figure 5. The Stoneley wave phase velocity, attenuation and amplitude are evaulated in the frequency range between 0.5 kHz and 3.0 kHz. The attenuation increases and phase velocity decreases as we go to lower frequencies reflecting the effects of a permeable formation (Schmitt et al., 1988).

Damped Least-Squares Inversion

The inversion problem can be set up using the Taylor expansion as:

$$D_i^o = D_i^c + \sum_{j=1}^{M} \frac{\partial D_i^c}{\partial P_j} \Delta P_j + O(\Delta P_j^2) \qquad (i = 1, 2, ..., N) \tag{3}$$

where D_i^o are observed data and D_i^c are calculated data with the initial model P_{jo}. P_j are parameters which describe the model. In our problem the observed data D_i^o consist of Stoneley wave velocity and attenuation estimated from the Prony's method analysis of the array waveform data. The inversion parameters can be shear wave velocity,

or permeability depending on what borehole model we used to do the inversion. The i represents the different frequencies with a total of N frequency points. The total number of inversion parameters is M. Here we approximate the partial derivatives in Eq. (3) by solving the period equation for the Stoneley wave for small changes in the parameters and then use finite differences in the resulting phase velocity and attenuation.

Eq. (3) can be linearized by dropping the $O(\Delta P_j^2)$ term and rewritten in a compact form:

$$\mathbf{Ax} = \mathbf{b}. \tag{4}$$

The damped least-square solution of (4) is given by:

$$\mathbf{x} = (\mathbf{A}^T\mathbf{A} + \varepsilon^2\mathbf{I})^{-1}\mathbf{A}^T\mathbf{b} \tag{5}$$

where ε^2 is the damping factor and $\mathbf{I}$ an identity matrix. The superscript T stands for transposition. The damping factor supresses the contribution of eigenvectors of matrix $\mathbf{A}^T\mathbf{A}$ whose eigenvalues are less than ε^2 (Aki and Richards 1980). The new value of P_j is

$$P_j = P_{jo} + \Delta P_j. \tag{6}$$

Eq. (6) gives us only an estimate of P_j, since we have linearized the inverse problem. To improve the estimate we use P_j as a new initial model and iterate the procedure until we obtain a satisfactory fit to the observations. Meanwhile at each iteration we reduce the damping factor ε. In this inversion procedure we can also make use of the amplitude information obtained from the data processing. The normalized amplitudes are used as a weighting function at different frequencies. The phase velocity and attenuation of the Stoneley wave at frequencies with large amplitudes are more reliable than those with small amplitudes.

One parameter of interest is formation permeability. The range of its magnitude is about a factor of 10^4 from core measurements. Here we adopt a logarithmic parameterization scheme in both the data and the model space to set up our inverse problem. Our original inversion problem consists of a set of linear equations (3) and update (Eq. 6). With logarithmic parameterization we have

$$\sum_{j=1}^{M} \frac{P_j \partial D_i}{D_i \partial P_j} \Delta \ln P_j = \ln \frac{D_i^o}{D_i}. \tag{7}$$

The new value of P_j is

$$P_j = P_{jo} \exp(\Delta \ln P_j). \tag{8}$$

One advantage of the logarithmic parameterization scheme is its ability to deal with large changes in the parameters in one iteration. In this case, changes in the permeability of one order of magnitude will only result in a change of unity in the actual parameter vector. This parameterization really helps in stabilizing the inversion and speeds up the convergence.

RESULTS AND DISCUSSIONS

Isotropic Borehole Model

This is the simplest borehole model. The fluid-filled borehole of radius R_0 is embedded in an isotropic solid formation and extends to infinity. The borehole is filled with a fluid of velocity V_f and density ρ_f. The compressional wave velocity of the formation is V_p, shear wave velocity V_s and density ρ_s. In a hard formation ($V_s > V_f$), the Stoneley wave phase velocity is less than V_f. In the soft formation ($V_s < V_f$), the phase velocity is less than V_s. It is slightly dispersive. Its amplitude decays exponentially in both the fluid and formation away from the borehole wall. The attenuation of the Stoneley wave is controlled by the quality factor of the fluid Q_f and of the formation shear wave Q_s.

The above described procedures of the data processing and inversion are applied to our two data sets using the isotropic borehole model. The borehole radius is 12.2 cm from the caliper log. The fluid compressional wave velocity is taken to be 1.5 km/s. Fluid and formation density are taken to be 1.1 g/cm^3 and 2.15 g/cm^3, respectively. The borehole fluid attenuation Q_f, formation P-wave attenuation Q_p and S-wave attenuation Q_s are obtained by trial and error to fit Stoneley wave attenuation data from 2.0 kHz to 3.0 kHz. They are 20, 50, and 25 respectively. The inversion parameter is the formation shear wave velocity. Data used in the inversion are the Stoneley wave phase velocities between 1.5 kHz and 3.0 kHz. The Stoneley wave amplitudes are normalized and used as a weighting function in the damped least-squares inversion. The formation P-wave velocity (V_p) is obtained directly from first arrivals of array data. The intial value of shear velocity is taken to be $V_p/1.7$.

The first data set is the data collected between depths of 2950 and 3150 ft. Inverted shear wave velocities are shown in Figure 6. The shear wave velocity from the dipole shear wave tool and the P-wave velocities from the array sonic tool are also shown in the figure. There is an excellent agreement between the inverted shear wave velocities and the shear wave velocities from the dipole tool. This agreement comes from the fact that in the slow formation the Stoneley phase velocity is very sensitive to the formation shear wave velocity.

The second data set is the data collected in the same borehole lower down at between depths of 3650 and 3850 ft. The interval consists of a shale cap section (at around 3690 ft) overlying a fractured and porous permeable sand (about 3700 to 3800). The inverted formation shear wave velocity, dipole measured shear wave velocity and the formation P-wave velocity are plotted in Figure 7. In this data set there is one section in the sand (3715 to 3780 ft) in which the inverted shear wave velocities disagree with the dipole shear wave velocities. This disagreement is beyond the errors in the measurements. The inverted shear wave velocity is lower than the dipole shear velocity. The core samples

indicate a high permeability (1 to 10 darcies) zone in this section. So our isotropic solid borehole model is not correct. The question then becomes: can the high permeability account for this difference in the shear wave velocities? This leads to our next model.

Porous Borehole Model

Biot(1956 a,b) proposed a theory of wave propagation in fluid-filled porous media. Rosenbaum (1974) applied the Biot model to the borehole geometry. The permeable borehole formation causes the Stoneley wave phase velocity to decrease and attenuation to increase, especially at low frequencies. Tang et al. (1991) formulated a simplified version of the Biot-Rosenbaum model to deal with Stoneley wave propagation in the permeable borehole.

For the second data set we consider a model of the borehole surrounded by a porous medium. We use the Stoneley wave phase velocity and attenuation at 530 Hz as the input data for the inversion and permeability as the inversion parameters. In the inversion we assume the open borehole wall condition. The inversion results of permeability from the Biot-Rosenbaum model are plotted against the core measurements in Figure 8. There is a good agreement between the two permeabilities. The inverted permeabilities clearly show the low and the high permeable zones. Inverted permeabilities also show the trend of the core measurements.

One effect of permeability on the Stoneley wave is to decrease its phase velocity. This may help to explain why the inverted shear wave velocities in the high permeability section (3715–3780 ft) are lower than the dipole measured ones. We reinverted for formation V_s using a porous formation borehole model, using the same 1.5 to 3.0 kHz Stoneley wave velocity data. In Figure 9 we plotted the inverted V_s from the porous and elastic models as a function of depth as well as the V_s from the dipole tool. The plot shows that there is little effect of permeability on inversion of formation shear wave velocity, although it did increase the inverted shear wave velocity by a small amount. This is because the permeability effect is restricted in the low frequency range and has little effect in our V_s inversion frequency range (1.5 to 3 kHz). So the permeability is not the cause of the disagreement of inverted V_s and shear wave log V_s.

Anisotropic Borehole Model

A possible interpretation of the difference in the shear wave velocities from the two tools is formation anisotropy. As discussed earlier, in a transversly anisotropic formation with the axis of symmetry in line with the borehole, the shear wave velocity measured by the dipole tool is the vertical shear wave velocity, while that measured by the Stoneley wave is the horizontal shear wave velocity (Ellefsen et al., 1991). In this case, as that

in a shale, the dipole shear wave velocity should be slower than the inverted one. This is confirmed in the shale section at around 3690 ft in the data.

In the permeable sand section, the problem is much more complicated. Here we have the dipole shear wave velocity higher than the inverted shear wave velocity, and the difference cannot be explained by the formation permeability. Our interpretation of this result is that the permeable formation is fractured. This fact was noted in the core description. Unfortunately no further description for the fractures was given. We are assuming that the fractures are subvertical, creating a situation where there is azimuthal anisotropy.

Under these assumptions, we can go ahead and interpret our results. In most cases, the dipole shear wave log measures the fastest velocity in the vertical direction, the exception being the case where the dipole is lined up in the slow azimuthal direction (Ellefsen et al., 1991). The Stoneley wave, on the other hand, measures a mixture of the fast and slow shear wave velocities. Under a zero frequency assumption, Rice (1987) stated that the Stoneley wave will measure the slow shear wave velocity. However, the numerical simulations of Ellefsen et al. (1991) showed that the Stoneley wave actually measures a weighted average of the fast and slow shear wave velocities, about a ratio of 2 to 1 for fast to slow, although the exact combination is not available at this time.

Using both the results of Rice (1987) and Ellefsen et al. (1991), and assuming that the dipole shear wave log measures the fast shear wave velocity, we can estimate the azimuthal shear wave velocity anisotropy in the fractured, high permeability section. Figure 10 shows the shear wave velocities estimated using the results of Rice (1987) and Ellefsen et al. (1991) and the resulting shear wave anisotropy. The degree of shear wave anisotropy seen in the permeable zone is around 5 to 15%, not unreasonable for a fractured rock.

There is one more check on the assumption of azimuthal anisotropy. In the full waveform data in the permeable zone (3700 to 3780 ft), there appears to be a "shear/pseudo-Rayleigh" wave arrival in front of the Stoneley wave (see Figure 2). Given the Stoneley wave velocity and the inverted shear wave velocity based on an isotropic elastic model, the formation is "slow" and there should not be a "shear/pseudo-Rayleigh" arrival. Despite this, we went ahead and estimated the phase velocity of this arrival using the semblance cross-correlation (Kimball and Marzetta, 1984; Block et al., 1991). The results are plotted in Figure 11 together with the dipole shear wave velocity and the inverted shear wave velocity from the Stoneley wave.

There are a couple of observations we can draw from Figure 11. If our hypothesis of azimuthal anisotropy is correct, then it appears that the observed arrival in the array sonic data does travel with the velocity of the fast shear wave velocity. Moreover, it gives the fastest shear wave velocity all along the fractured sandstone section. This understandable since its frequency is around 6 kHz as opposed to the 2 kHz flexural

wave generated by the dipole tool. Thus the dipole tool may tend to average the surrounding slower velocities in the formation. Furthermore, this arrival travels with a velocity greater than the 1500 m/s, thus supporting the idea that this is some sort of a "refracted shear/pseudo-Rayleigh" arrival.

A second observation is that the dipole shear wave tool does not always measure the fastest shear wave velocity. It is evident that above around 3710 ft the dipole is tracking the "slow" shear wave velocity while the "refracted shear" arrival in the array sonic is actually tracking the "fast" shear wave velocity in this fractured sandstone formation. Below 3710 ft the dipole shear wave log starts to track the "fast" arrival, although for the most part it is still a little slower than that from the array sonic, probably because of the lower frequency content. This is probably the result of tool rotation in the dipole tool. This also points out the importance of a combined integrated interpretation of both the full waveform array sonic and the dipole log. Using only one or the other could lead to an erroneous interpretation.

CONCLUSIONS

Borehole Stoneley wave phase velocity and attenuation obtained from processing array full waveform log data and shear wave velocity from the dipole log can be used together to estimate formation parameters. In an isotropic elastic borehole the inverted V_s from Stoneley wave phase velocity is in excellent agreement with the shear wave log result. Estimated formation permeabilities from low frequency Stoneley wave velocity and attenuation data are in good agreement with the core measurements. The shear wave velocity from the inverted Stoneley wave velocity can be used in combination with the dipole shear wave velocity and possible "refracted shear/pseudo-Rayleigh" wave arrival in the array sonic data to indicate formation shear wave anisotropy.

ACKNOWLEDGEMENTS

REFERENCES

Biot, M.A., 1956a, Theory of propagation of elastic waves in a fluid saturated porous rock: I. Low frequency range; *J. Acoust. Soc. Am.,* *28,* 168–178.

Biot, M.A., 1956b, Theory of propagation of elastic waves in a fluid saturated porous rock: II. Higher frequency range; *J. Acoust. Soc. Am.,* *28,* 179–191.

Block, L.V., C.H. Cheng, and G.L. Duckworth, 1991, Velocity analysis of multi-receiver full waveform acoustic logging data in open and cased holes, *The Log Analyst, 32,* 188–200.

Burns, D.R., C.H. Cheng, D.P. Schmitt, and M.N. Toksöz, 1988, Permeability estimation from full waveform acoustic logging data; *The Log Analyst, 29,* 112–122.

Cheng, C.H., and M.N. Toksöz, 1981, Elastic wave propagation in a fluid-filled borehole and synthetic acoustic logs; *Geophysics, 46,* 1042–1053.

Cheng, C.H., and M.N. Toksöz, 1983, Determination of shear wave velocities in "slow" formation, *Trans. SPWLA 24th Ann. Logging Symp.,* Calgary, Canada, Paper V.

Ellefsen, K.L., 1990, Elastic wave propagation along a borehole in an anisotropic medium; Ph.D. Thesis, Massachusetts Institute of Technology, Cambridge, Mass. ,

Ellefsen, K.L., C.H. Cheng, and K.M. Tubman, 1989, Estimating phase velocity and attenuation of guided waves in acoustic logging data; *Geophysics, 54,* 1054–1059.

Ellefsen, K.L., C.H. Cheng, and M.N. Toksöz, 1991, Effects of anisotropy upon the normal modes in a borehole, *J. Acoust. Soc. Am., 89,* 2597–2616.

Gibson, R.L., and, M.N. Toksöz 1990, Permeability estimation from velocity anisotropy in fractured rock; *J. Geophys. Res., 95,* 15643-15655.

Kimball, C.V., and T.L. Marzetta, 1984, Semblance processing of borehole acoustic array data, *Geophysics, 49,* 274–281.

Lang, S.W., A.L. Kurkjian, J.H. McClellan, C.F. Morris, and T.W. Parks, 1987, Estimating slowness dispersion from arrays of sonic logging data; *Geophysics, 52,* 530–544.

Nur, A.M., 1969, Effects of stress and fluid inclusions on wave propagation in rock; Ph.D. Thesis, Massachusetts Institute of Technology, Cambridge, Mass.

Rosenbaum, J.H., 1974, Synthetic microseismograms: logging in porous formations; *Geophysics, 39,* 14–32.

Rice, J.A., 1987, A method of logging shear wave anisotropy, *57th SEG Ann. Mtg. Expanded Abstracts*, 27–28.

Schmitt, D.P., 1986, Full wave synthetic acoustic logs in saturated porous media: Part I,II,III; *M.I.T. Full Waveform Acoustic Logging Consortium Annual Report* 105–330.

Schmitt, D.P., M. Bouchon, and G. Bonnet, 1988, Full-wave synthetic acoustic logs in radially semi-infinite saturated porous media, *Geophysics, 53*, 807–823.

Stevens, J.L., and S.M. Day, 1986, Shear velocity logging in slow formations using the Stoneley wave, *Geophysics, 51*, 137–147.

Tang, X.M., C.H. Cheng, and M.N. Toksöz, 1991, Dynamic permeability and borehole Stoneley waves: A simplified Biot-Rosenbaum model, *J. Acoust. Soc. Am., 90*, 1632–1646.

White, J.E., and C. Tongtaow, 1981, Cylindrical waves in transversely isotropic media; *J. Acoust. Soc. Am., 70*, 1147–1155

Williams, D.M., J. Zemanek, F.A. Angona, C.L. Dennis, and R.L. Caldwell, 1984, The long space acoustic logging tool; *Trans. SPWLA 25th Ann. Logging Symp.*, Paper T.

Winkler, K.W., H.L. Liu, and D.L. Johnson, 1989, Permeability and borehole Stoneley waves: comparison between experiment and theory; *Geophysics, 54*, 66–75.

Zemanek, J., F.A. Angona, D.M. Williams, and R.L. Caldwell, 1984, Continuous acoustic shear wave logging, *Trans. SPWLA 25th Ann. Logging Symp.*, New Orleans, Paper U.
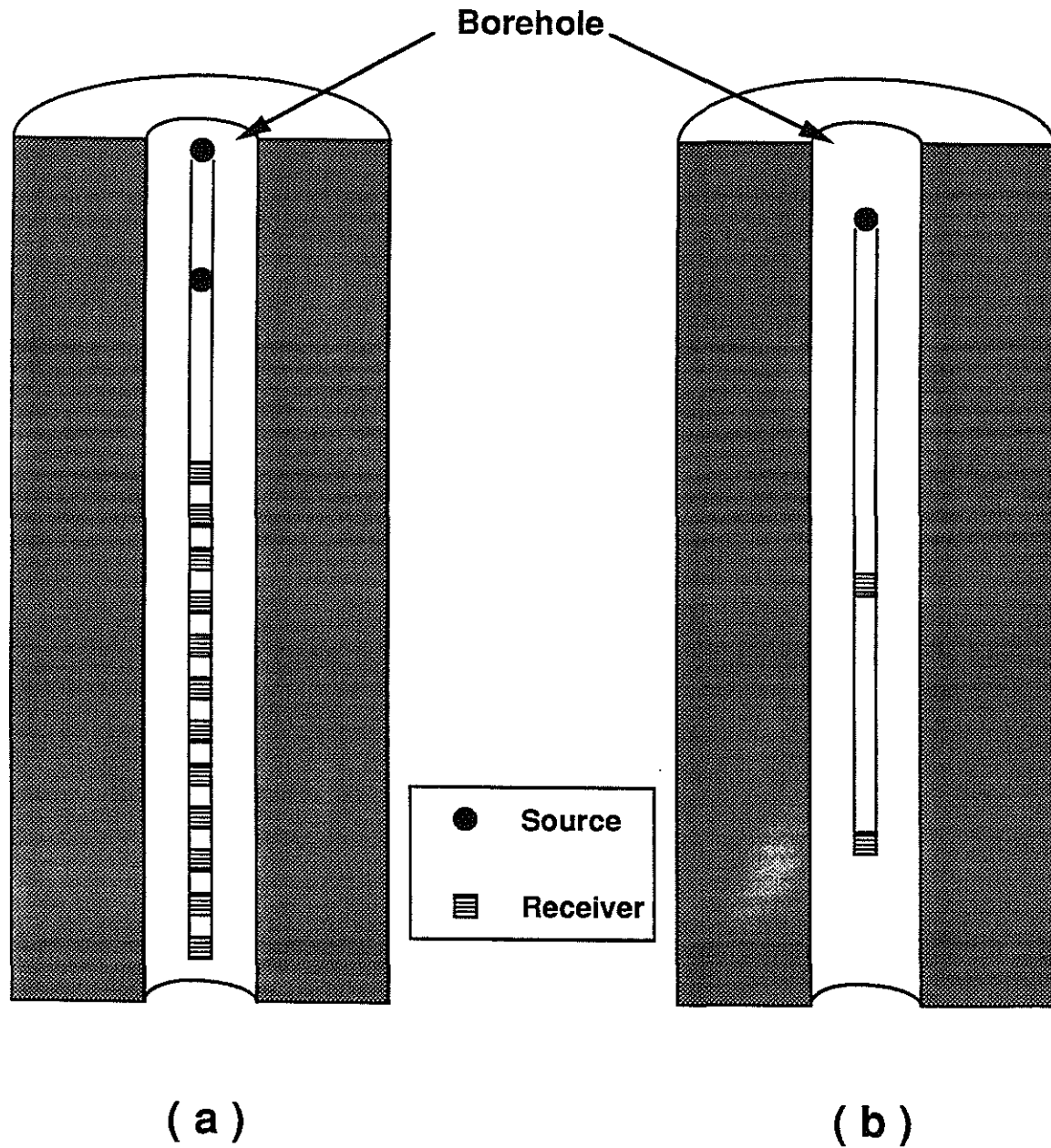
Figure 1: Schematic diagram of the source/receiver arrangement for the Arco full wave-
form array sonic logging tool and the Arco shear wave logging tool.
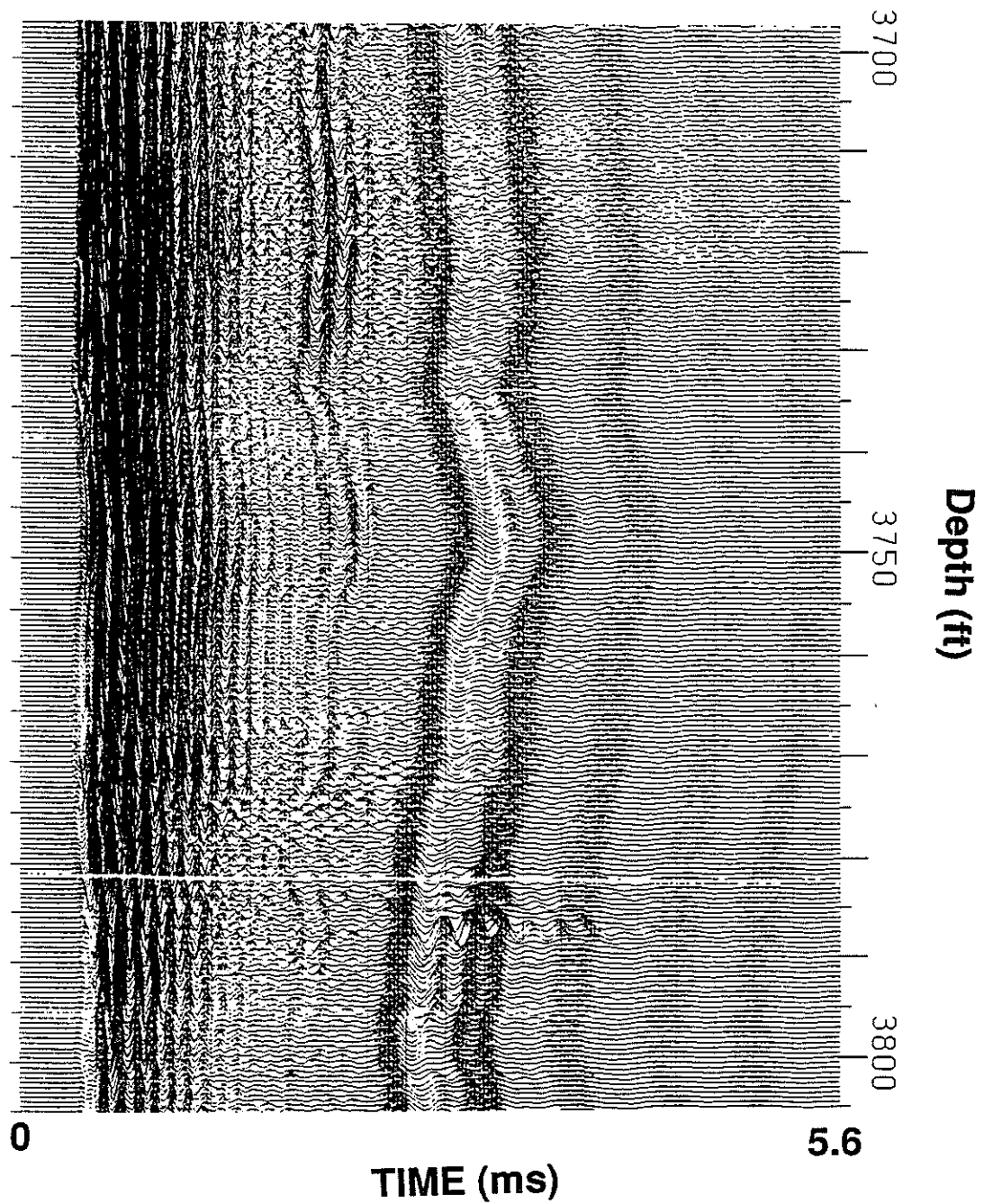
Figure 2: Iso-offset section of the full waveform sonic logging data from a section of the data set used in this study.
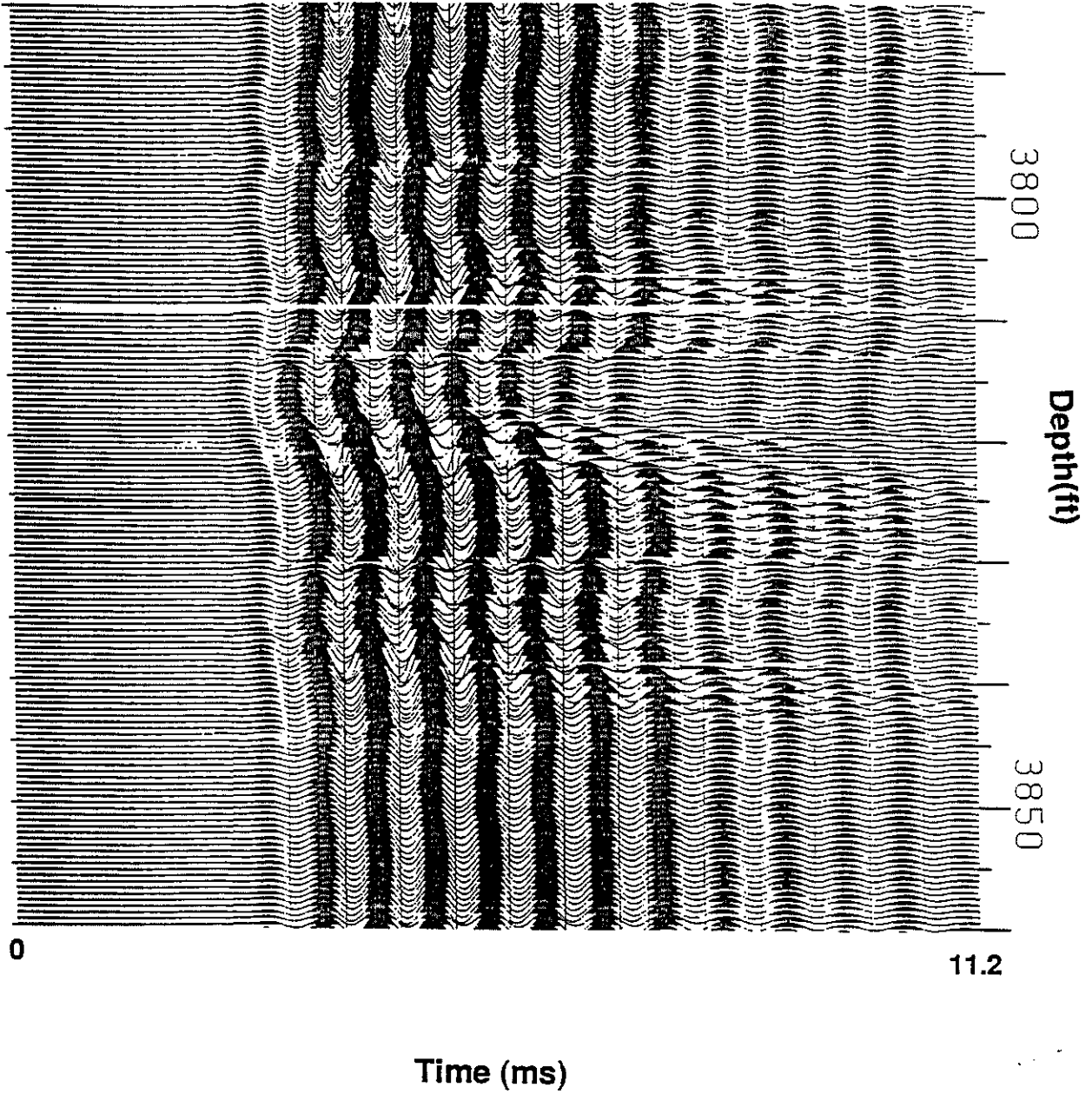
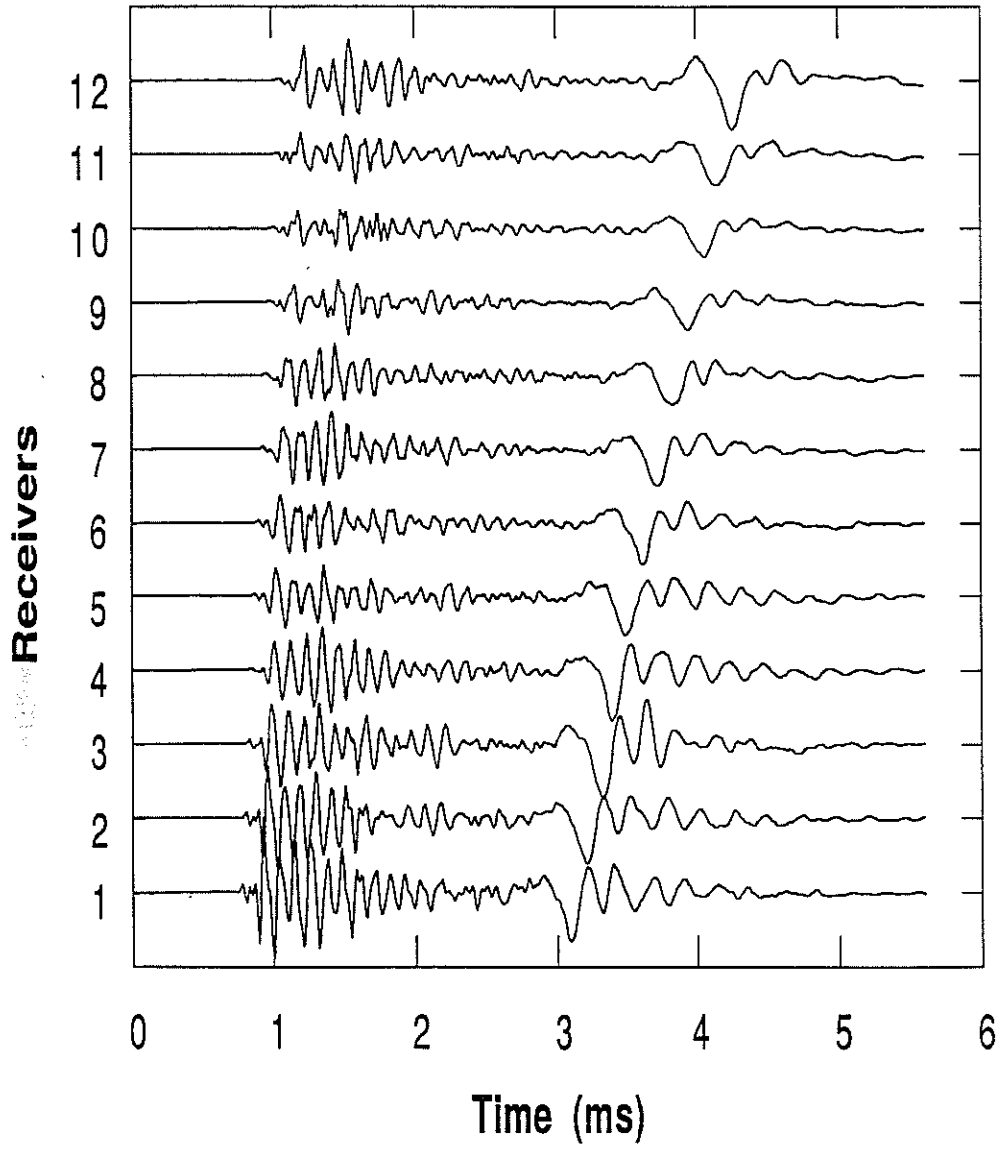Figure 3: Iso-offset section of the shear wave logging data.

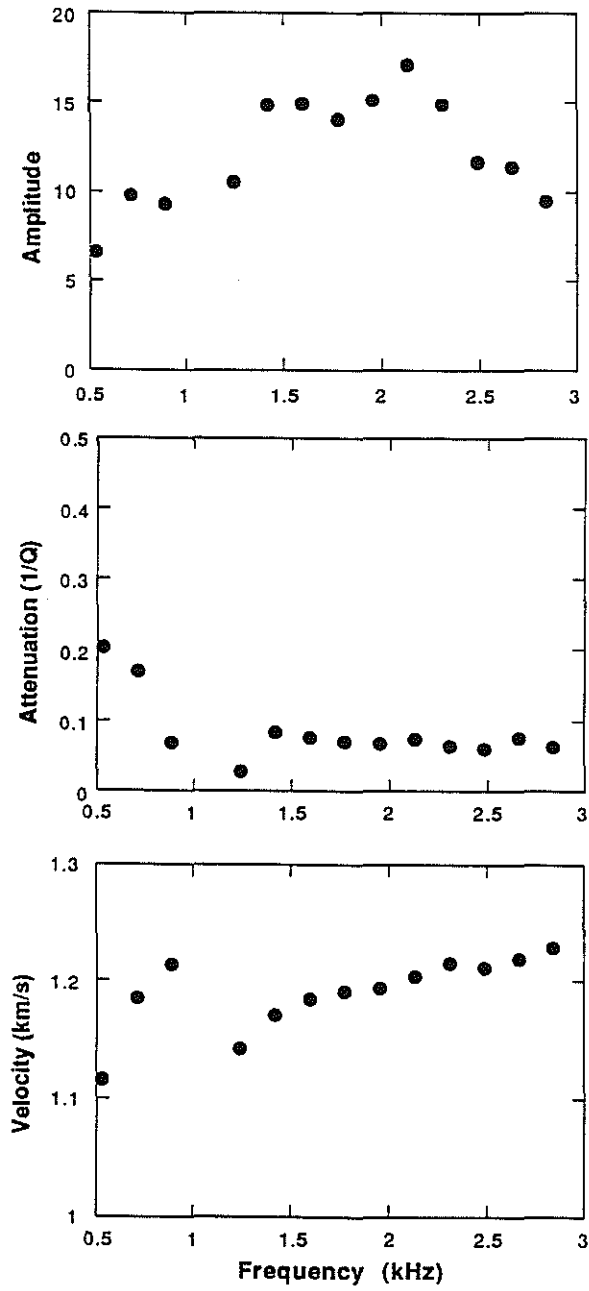Figure 4: Representative data from various receivers in the array sonic tool.

Cheng and Cheng

Figure 5: An example of the amplitude, phase velocity and attenuation of the Stoneley wave as a function of frequency.
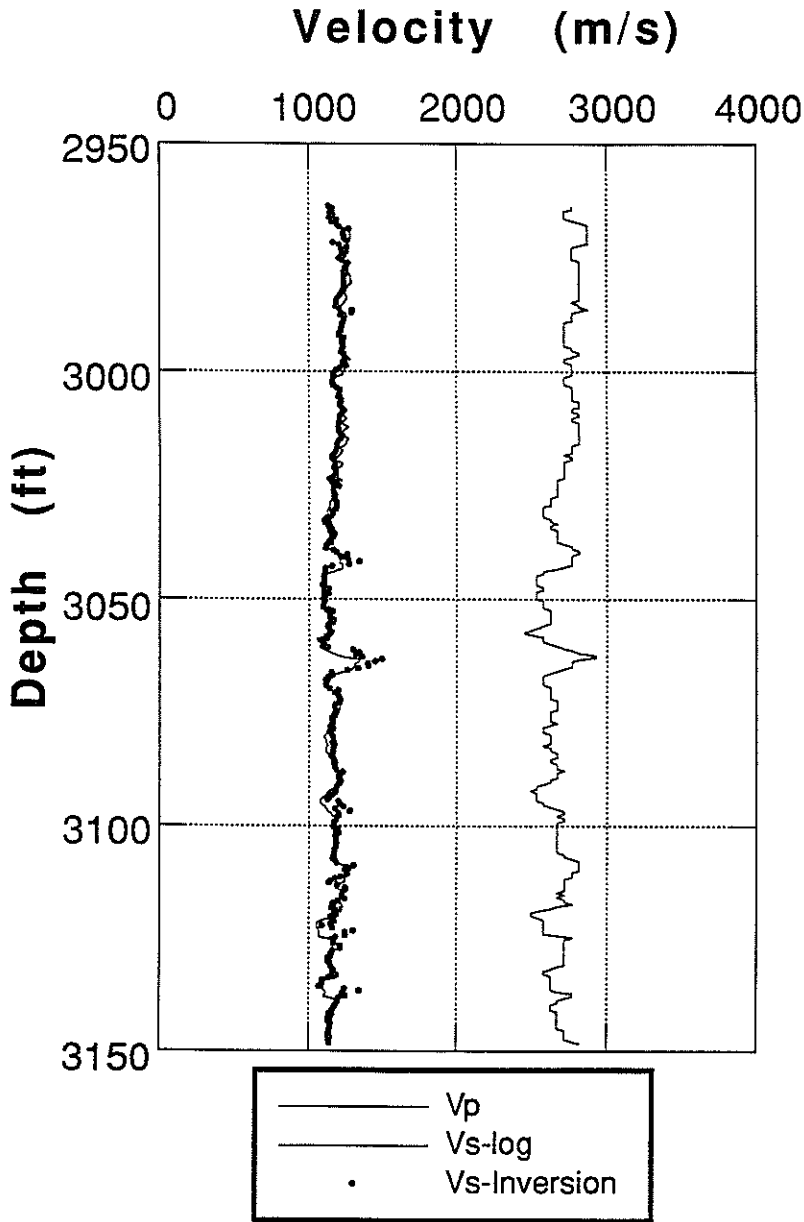
Figure 6: Inversion results for the upper portion of the borehole. The formation V_s from inverted Stoneley wave velocity is shown with the shear wave log V_s. The formation V_p is also shown.
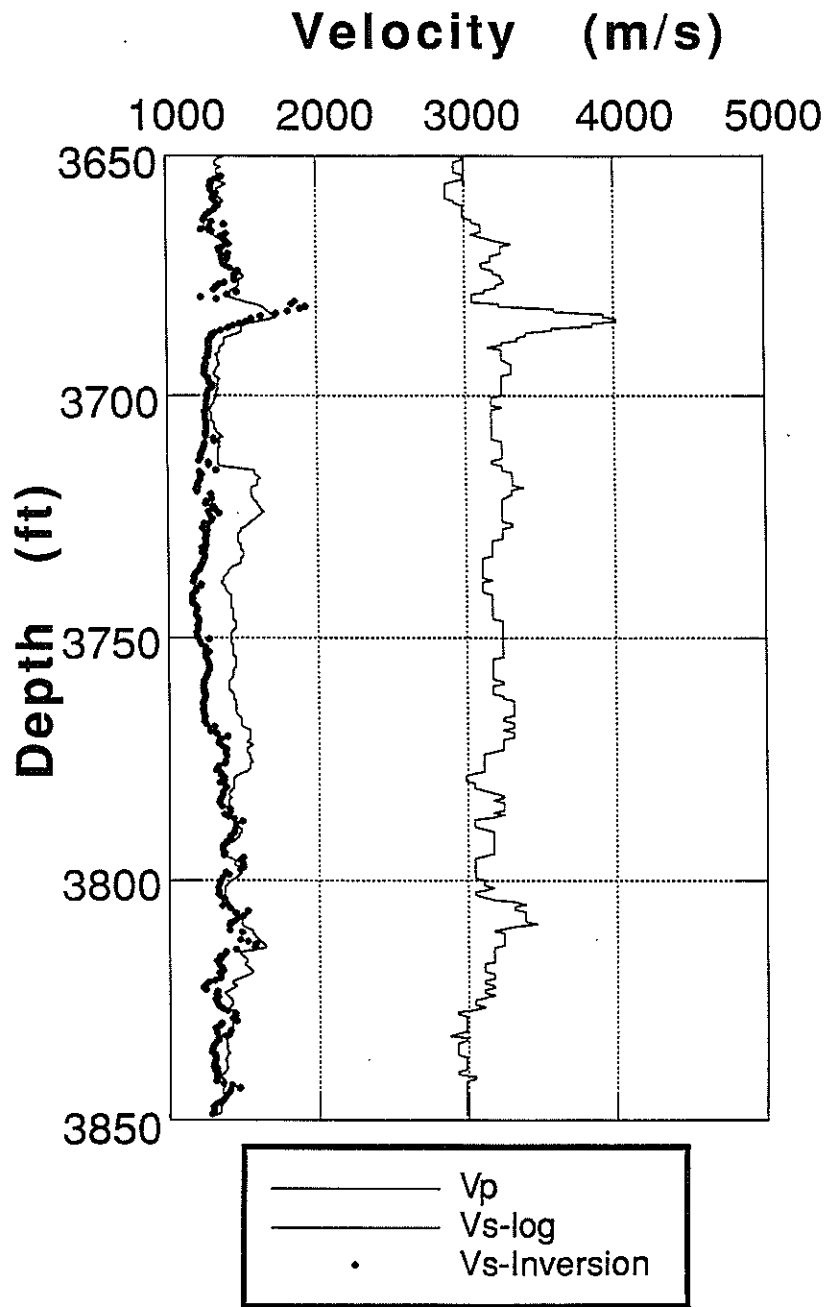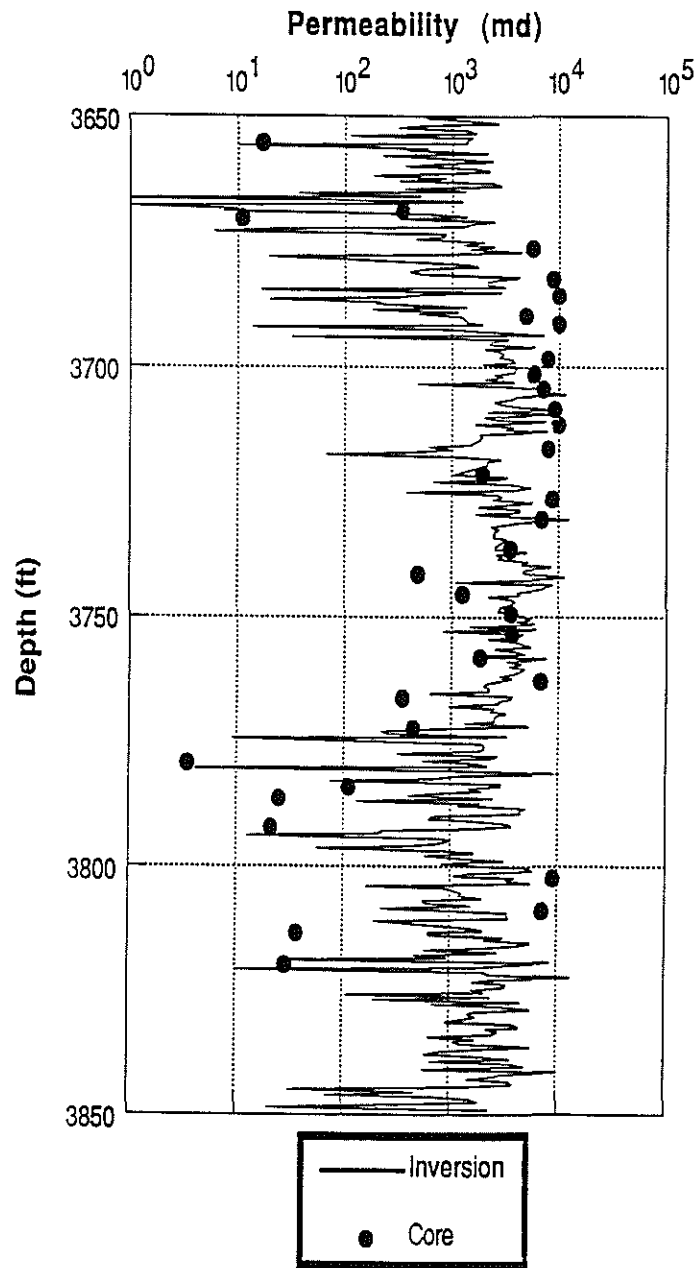
Velocity (m/s)

Figure 7: Inversion results for the lower portion of the borehole. The formation V_s from inverted Stoneley wave velocity is shown with the shear wave log V_s. The formation V_p is also shown.

Figure 8: Inverted permeability using the Biot-Rosenbaum model (solid line) versus core measurements (open circles).
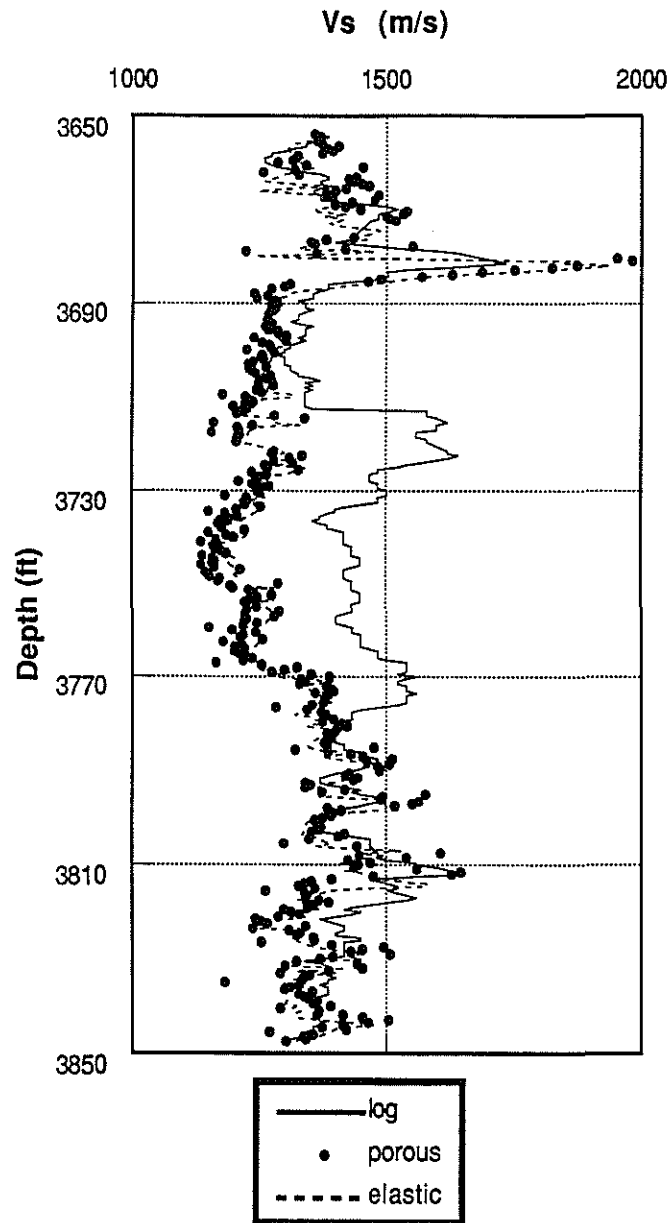
Figure 9: Inversion results for the formation V_s from the porous formation model and the elastic model compared with shear wave log V_s.
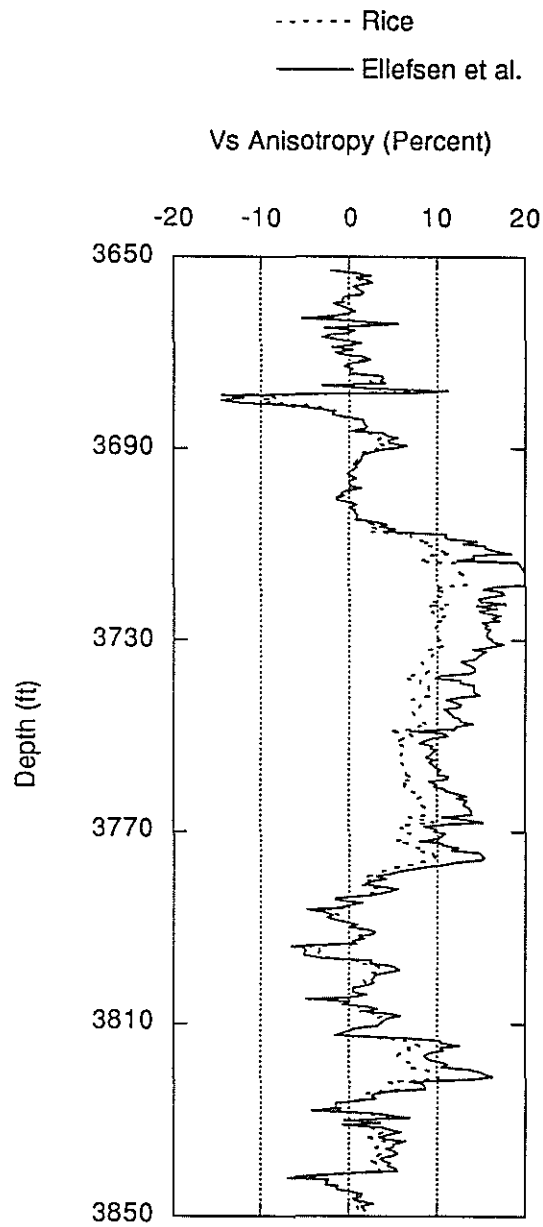
Figure 10: Shear wave anisotropy determined using the Rice (1987) and the Ellefsen et al. (1991) assumptions.
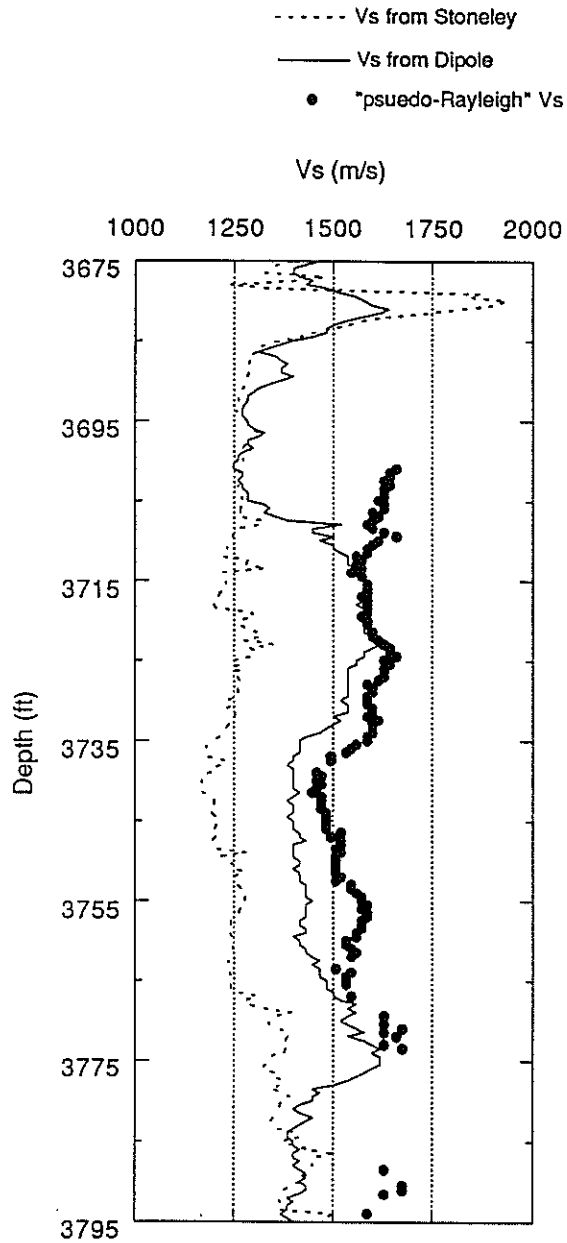
Figure 11: Shear wave velocity determined from inverted Stoneley wave velocity as compared with V_s from the dipole tool and the velocity from the "refracted shear/pseudo-Rayleigh" arrival in the array sonic data.